15 Gbps 50 cm Wireless Link Using a High Power Compact III-V 84 GHz Transmitter

Jue Wang, Abdullah Al-Khalidi, Liquan Wang, Razvan Morariu, Afesomeh Ofiare and Edward Wasige

***Abstract*—The paper reports on a 15 Gbps wireless link that employs a high power resonant tunneling diode (RTD) oscillator as a transmitter. The fundamental carrier frequency is 84 GHz and the maximum output power is 2 mW without any power amplifier. The reported performance is over a 50 cm link, with simple amplitude shift keying (ASK) modulation utilized. The 15 Gbps data link shows correctable bit error rate (BER) of 4.1×10^{-3}, while lower data rates of 10 Gbps and 5 Gbps shows BER of 3.6×10^{-4} and 1.0×10^{-6}, respectively. These results demonstrate that the RTD transmitter is a promising candidate for the next generation low cost, compact, ultra-high data rates wireless communication systems.**

***Index Terms*—resonant tunneling diode, wireless communication systems, amplitude shift keying, oscillator, high power transmitter.**

I. Introduction

With the development of modern multimedia technology there is great demand for ultra-high speed wireless communication. The typical application scenarios include wireless local area networks (WLAN), wireless personal area networks (WPAN), kiosk downloading, wireless connection in data centers, chip to chip interconnects, wireless backhauling, nano cells, etc. Based on extrapolation of Edholm's law and future demand analysis, the data rate in the near future is expected to reach about 100 Gbps [1]–[3].

For current wireless communication systems operating in the low microwave range, a great challenge consists of the fundamental limitation of the narrow bandwidth, despite efforts to improve spectral efficiency by using advanced modulation schemes and signal processing techniques. Therefore, many candidate technologies for future wireless systems operate in the higher bands where wider bandwidth is available.

The resonant tunneling diode (RTD) is the fastest solid state device compared to any other traditional electronic devices such as field effect or bipolar transistors (MOSFETs, HEMTs or HBTs), or diode technologies (IMPATT, Gunn, etc.). The fundamental frequency of an RTD oscillator is approaching 2 THz [4].

Recently, high data rate wireless transmission using RTDs has been reported. Asada's group achieved 30~34 Gbps data rates by using direct modulation of the RTD using amplitude shift keying (ASK). The transmitter comprised a single 1 μm^2 sized RTD in slot antenna. High peak current density, >600 kA/cm^2, RTD epitaxial designs were used. The transmitter frequency was 490 GHz with 26~60 μW output power [5][6]. Due to the high dielectric constant of the substrate, the radiated power is directed mostly in the substrate and is therefore extracted from the substrate backside through a Si-collimation lens. Earlier, Ohlsson *et al*. reported a 15 Gbps over 1.5 m wireless link using an RTD-MOSFET wavelet generator [7]. A 62.5 GHz single RTD source with 3.2 mW output power was integrated with 130 nm III-V MOSFET switch through which the source was modulated. A horn antenna was used in this setup. The group have also employed a dielectric resonator antenna in [8]. This approach is, however, limited to using only on-off keying (OOK) modulation scheme.

In this paper, we propose a high power (2 mW) W-band double RTD MMIC transmitter design. The work reported here is based on our earlier research which has established a robust mm-wave and terahertz RTD source technology [9]-[12]. The designs feature low phase noise sources [9] and relatively high output powers of around 1 mW, 0.5 mW and 0.3 mW at W-band, D-band and J-band, respectively [10]-[12]. A unique feature of the approach is the use of low peak current density, ~190 kA/cm^2, epitaxial designs and therefore large mesa RTD sizes of around 9 – 25 μm^2. The device self-capacitance is in the femtofarad range, ~3 fF/μm^2, and so requires only a suitably chosen resonating inductance to realise the required frequency.

The transmitter reported here was designed for high speed short range wireless communication applications. The modulation scheme employed was ASK. OOK, as a special case of ASK, was also investigated. High data rates of 15 Gbps with over 50 cm long wireless links was demonstrated. The preliminary results show comparable/better performance than most up to date Si-based CMOS transceiver solutions. In Refs. [13] [14], for instance, 60 GHz carrier frequencies using 90 nm CMOS are demonstrated using OOK modulation with corresponding 3.3 Gbps/10.7 Gbps data rates over 4 cm/10 cm ranges. In [15], 80/100 GHz transceiver using 65 nm CMOS is demonstrated using ASK modulation at 23 Gbps over a 1 cm wireless link. In [16], a 57/80 GHz transceiver using 40 nm CMOS shows ASK modulated 20 Gbps over a 5 mm wireless

"This work was supported by European Commission, grant agreement no. 645369 (iBROW project) and NSFC 61405110"

Jue Wang, Abdullah Al-Khalidi, Razvan Morariu, Afesomeh Ofiare and Edward Wasige are with the High Frequency Electronics group, University of Glasgow, UK. (e-mail: edward.wasige@ glasgow.ac.uk).

Liquan Wang is currently working with Shanghai Electro-Mechanical Engineering Institute, 3888 Yuanjiang Road, Shanghai, China.

TABLE I
PERFORMANCE COMPARISON

Reference	[13]	[14]	[15]	[16]	[6]	[7]	This work
Technology	90 nm CMOS	90 nm CMOS	65 nm CMOS	40 nm CMOS	1 μm² RTD	35 μm²-130nm RTD-MOSFET	16 μm² RTD
Frequency	60GHz	60GHz	80/100 GHz	57/80 GHz	490GHz	62.5 GHz	84 GHz
Modulation	OOK	OOK	ASK	ASK	ASK	OOK	ASK
Power Dissipation	Tx: 183 mW Rx: 103 mW	Tx: 31 mW Rx: 36 mW	Tx: 29 mW Rx: 78 mW	Tx: 52 mW Rx: 85 mW	N/A	Tx: 22 mW Rx:2.92 W	Tx: 114 mW Rx: 600 mW*
Tx (power)	5.8 mW	3.2 mW	0.3 mW/0.2 mW	0.5 mW	60 uW	3.2 mW	2 mW
PA(Gain)	9.6 dB	9.1 dB	yes	6 dB	No	No	No
Antenna type	Folded Dipole	Yagi	Yagi	Yagi/Dipole	Slot	Horn	Horn
Antenna gain	5.5 dBi	6.6 dBi	9 dBi	9/4.3 dBi	Not specified	20 dBi	21 dBi
Data rate	3.3Gbps	10.7Gbps	23 Gbps	20 Gbps	34Gbps	10/15Gbps	15 Gbps
Distance	600 mm	100 mm	20/10 mm	5 mm	5 mm	1.5m	500 mm

* zero bias SBD detector was used. Most Rx DC power was consumed by LNA.

link. This comparison is summarized in Table I. Compared with standard CMOS techniques, the RTD transmitter solution proposed in the paper does not require any power amplifier (PA) or frequency multiplier/synthesizer stage, which greatly reduces the circuit complexity and design costs. In addition, the described approach is applicable at higher frequencies also, as recently demonstrated by the group at 300 GHz targeting real emerging applications such as wireless data centres [17]. Last but not least, the RTD manufacture requires only low-cost photolithography because of the relaxed (μm) device geometry requirements. The proposed transmitter is therefore a very promising technique for future low-cost high speed wireless communication links.

The paper is organized as follows. Section II describes the wireless system architecture. Section III introduces the RTD transmitter design, including RTD device technology, device modeling and high power transmitter design. Section IV describes the wireless measurements and results, while section V provides conclusions of the work.

II. Wireless System Architecture

A. RTD Device characteristic and modulation scheme

The core layer structure of an RTD device consists of a narrow band gap (E_g) semiconductor material sandwiched between two thin wide bandgap materials. The epilayer is therefore called a double barrier quantum well (DBQW) structure. Electrons can tunnel through these barriers despite having lower self-energy [18], therefore the current-voltage (IV) characteristic of an RTD device exhibits a negative differential resistance (NDR) as shown in Fig. 1. By using this NDR feature, high frequency RTD oscillators can be designed. The RTD design details are introduced in section III. Both ASK and OOK modulation are applicable to the RTD transmitter depending on the bias position and the amplitude of data as illustrated in Fig. 1. ASK modulation has been widely used because of the advantages of being a simple, low cost, high bandwidth efficiency technique [19]. OOK as a special case of ASK represents the data modulation by switching on-off the carrier, and has been investigated as an alternative scheme. For OOK modulation, the RTD is biased near the peak voltage (V_p) position for input NRZ data to switch on-off the oscillator while for ASK modulation, RTD device is biased in the middle of NDR region. In contrast of OOK, the data amplitude requirement for ASK is low within NDR region as illustrated in Fig. 1.

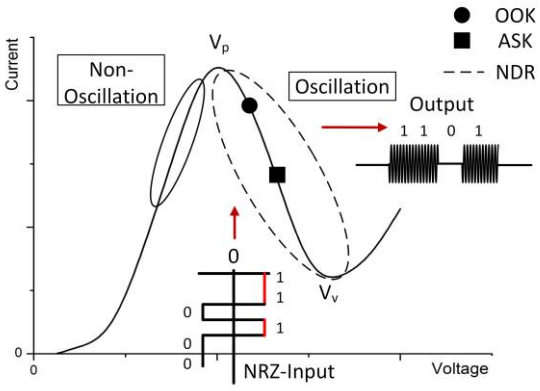

Fig. 1. Typical RTD device IV characteristics and illustration of ASK /OOK modulation.

B. Wireless system architecture

The block diagram of the wireless system is illustrated in Fig. 2.

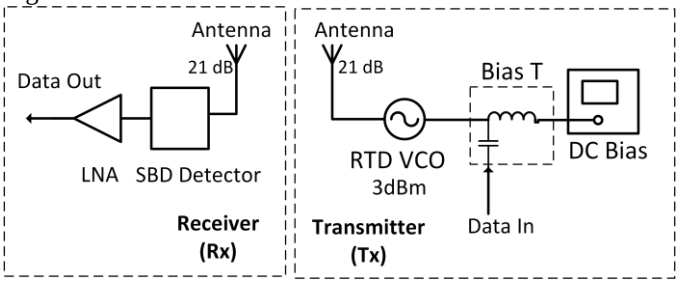

Fig. 2. Block diagram of the wireless system architecture.

The transmitter (Tx) consists of an 84 GHz (fundamental frequency) voltage controlled RTD oscillator (RTD-VCO) and WR-10 conical horn antenna. The data is superimposed over DC bias through a bias tee. As output power of RTD-VCO is high in mW range, no PA is employed in this stage. On the receiver (Rx) side, the identical WR-10 conical horn antenna is used. The signal is demodulated by a Schottky barrier diode (SBD) envelope detector and amplified by a low noise

amplifier (LNA).

C. Link budget

The measured transmitter output power is 3 dBm (2 mW); the antenna gain is 21 dBi (as given by the manufacturer data sheet) and is the same for both Tx and Rx; the total link loss is estimated to be 5 dB from Tx side and includes connection loss between the antenna and oscillator (2 dB), RF probe insertion loss (2 dB) and bias tee loss (1 dB). The Rx loss include the connection and cable loss value is assumed to be 2 dB in total. Insertion losses due to impedance mismatching of the antenna and oscillator output and miscellaneous losses are not considered in this experiment. For the SBD working in square-law detection region, the required power is in the range of 3-5 μW [20]. Therefore, given the transmitter power, the calculated maximum allowable free space path loss is 63 dB which corresponds to a distance of around 40 centimeters at 84 GHz.

III. TRANSMITTER DESIGN

A. Resonant tunneling diode (RTD) device

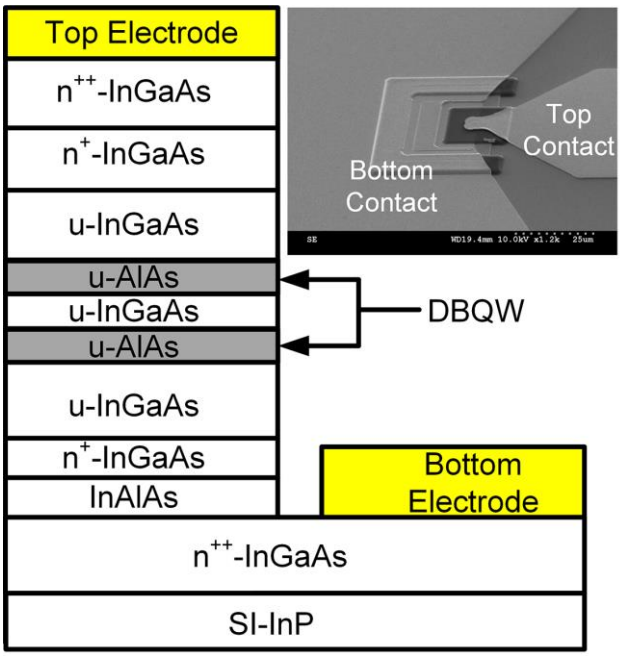

Fig. 3. Schematic layer structure of a RTD. The inset SEM picture shows the fabricated 16 μm^2 (top mesa) sized device.

The RTD epitaxial layer structure for this work consists of a 4.5 nm InGaAs quantum well (E_g = *0.75 eV*) sandwiched between double 1.4 nm AlAs barriers (E_g = *2.16 eV*). The typical RTD layer structure is shown in Fig. 3. The spacer layer is 26 nm for both collector and emitter. The inset scanning electron microscope (SEM) micrograph shows the central top contact mesa size of 16 μm^2. The fabrication process used for the presented devices is fully compatible with low cost optical lithography. Due to anisotropic wet etching (100 nm/min), the effective device size is estimated to be 12.8 μm^2 for the typical mesa height of 400 nm. The IV characteristic of the device is shown in Fig. 4. Due to parasitic bias oscillations, the measured I-V is distorted and shows a plateau-like feature in the NDR region. The peak current density is 187 kA/cm^2 and the peak to valley current ratio (PVCR) being about 2.5. The IV characteristic was modeled by using a 9th order polynomial which shows a good fit with the measurement. It was also modelled with a quasi-physical model in which with numerical constants are determined empirically [21]. Either of these analytical models are easy to use in circuit simulators. The calculated differential conductance (G_n) is also shown in Fig. 4. The NDR region is between peak voltage V_p = 0.9V and valley voltage V_v = 1.7V, with a minimum value of G_n of -42.5 mS.

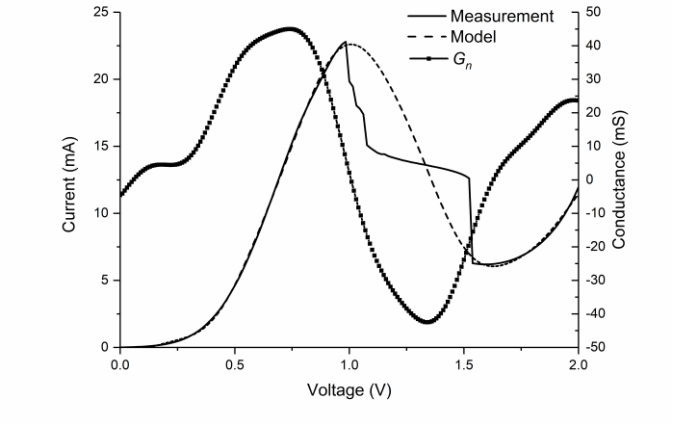

Fig. 4. Measured and modeled device IV characteristics. The negative differential conductance G_n is also shown. Note that the G_n is negative across the entire NDR region with a minimum value of -42.5 mS.

B. RTD device modeling

In order to realise an accurate oscillator circuit design, the RTD small signal model parameters were investigated. The RTD was represented by its small-signal RLC model as shown in Fig. 5.

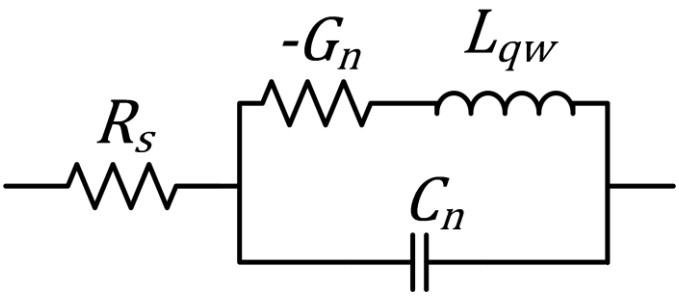

Fig. 5. RTD device RLC model. R_s represents the device series resistance, $-G_n$ the negative differential conductance and C_n the RTD capacitance. And L_{QW} is the quantum well inductance.

R_s represents the device series resistance including metal-semiconductor contact resistance and sheet resistance. As the contact layer doping level is high and a chosen small thickness of 40nm, the sheet resistance is negligible. The metal-semiconductor contact resistance is estimated from transmission line measurements (TLM). The measured value R_s is 5.2 Ω. $-G_n$ represents the negative differential conductance, which is calculated/extracted from both DC and S-parameter measurements. C_n denotes the RTD self-capacitance and includes the geometrical capacitance C_0 and quantum capacitance C_Q [22][23]. C_n as a crucial parameter, which

determines the oscillator frequency and is defined by (1) in terms of C_0 and C_Q. The geometrical capacitance C_0 can be estimated by (2), where A is the device size, L_W, L_B and L_D is the width of quantum well, barrier and depletion region respectively, ε_W, ε_B, and ε_D is the dielectric constant of quantum well, barrier and depletion region. The calculated $C_0 = 38$ *fF*. The quantum capacitance C_Q is estimated by (3) where v_C is the electron escape rate which is the reciprocal of the transit time (τ_{RTD}). It includes transit through quantum well (τ_{dwell}) and collector depletion region (τ_{dep}).

$$C_n = C_0 + C_Q \tag{1}$$

$$C_0 = \frac{A}{\frac{L_W}{\varepsilon_W} + \frac{2L_B}{\varepsilon_B} + \frac{L_D}{\varepsilon_D}} \tag{2}$$

$$C_Q = \frac{-G_n}{v_C} \tag{3}$$

C_Q was estimated to be 30 fF. The quantum-well inductance L_{QW} can be expressed in terms of electron dwell time (τ_{dwell}) in quantum well as [22][24]

$$L_{QW} = \frac{\tau_{dwell}}{G_n} \tag{4}$$

However, L_{QW} will not limit the oscillator frequency as discussed in Ref. [25]. Therefore, L_{QW} is neglected in the analysis. The intrinsic cut-off frequency (f_{int}) of the RTD is given by [26]

$$f_{int} = \frac{1}{4(\tau_{dwell} + \frac{\tau_{dep}}{2})} \tag{5}$$

τ_{dep} is estimated to be 87 fs for the 26 nm thick spacer (assuming a drift velocity of 3×10^7 cm/s [26]), while τ_{dwell} is estimated to be 618 fs from quantum capacitance C_Q. Therefore, f_{int} is about 378 GHz.

One port S-parameter measurements were taken in order to extract the capacitance value. The schematic of the measurement setup is shown in Fig. 6(a). The port input power was carefully chosen to ensure the RTD operated in its linear regime. The VNA output power was set at -33 dBm which is equivalent to 14 mV peak-peak voltage assuming 50 Ω load impedance. The coplanar waveguide (CPW) feed line with a characteristic impedance Z_0 = 50 Ω, length l = 100 μm was de-embedded by using open-short de-embedding method. The parasitic elements introduced by the CPW were represented by its lumped model as shown in Fig. 6(b). By subtracting Y parameter (Y_p) of the open structure and Z parameter (Z_s) of the short structure from measurement, the RTD capacitor value is derived from the imaginary part of Y_{11}. The specific values were extracted at 10 GHz at various bias points [27]. The results are plotted in Fig. 7. As the device is not stable in NDR, no valid data could be obtained in this region. The extracted C_n value is about 40 fF (Fig.7). This value is consistent with the geometrical capacitance value in the positive differential resistance region.

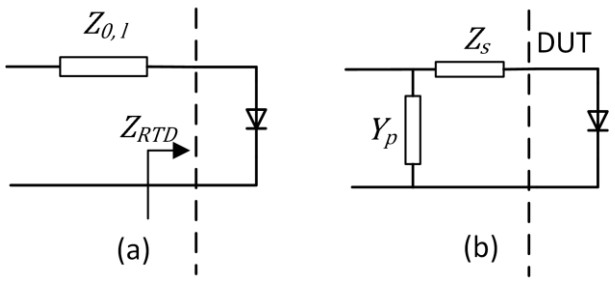

Fig. 6. (a) Schematic de-embedding circuit and (b) Equivalent lumped model including admittance Y_p and impedance Z_s..

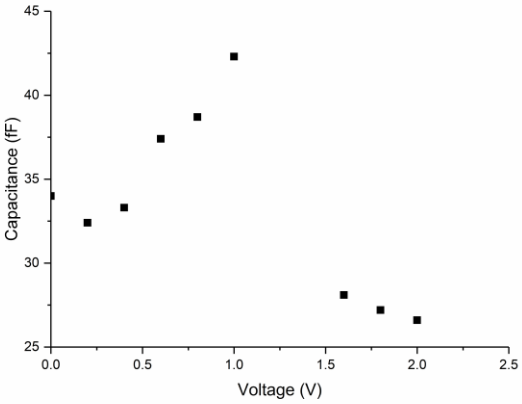

Fig. 7. Extracted capacitance value of the 16 μm² sized RTD device. The capacitance is bias voltage dependant.

The impedance of the device Z_{RTD} is presented by (6):

$$Z_{RTD} = R_s - \frac{G_n + j\omega C_n}{G_n^2 + (\omega C_n)^2} \tag{6}$$

The cutoff frequency is derived by (7) when the real part of Z_{RTD} equals zero:

$$f_{max} = \frac{1}{2\pi C_n}\sqrt{\frac{G_n}{R_s} - G_n^2} \tag{7}$$

The calculated cut-off frequency of the 16 μm² sized RTD is 325 GHz.

C. Double RTD oscillator design and measurement

Compared to the commonly employed single RTD slot antenna design, whose radiation pattern is measured through a hemispherical Si lens, e.g. [4][28], the high power RTD oscillator design proposed here employs two RTDs in parallel in an on-wafer configuration. The schematic circuit diagram of the oscillator is shown in Fig. 8 (a), where R_e is the stabilizing resistor to suppress the low frequency bias oscillations. The bypass capacitor C_e is included in order to short the RF signal to ground at the designed oscillation frequency. Inductor L is designed to resonate with the RTDs' self-capacitance in order to determine the oscillating frequency. R_L is the load resistance. As two devices are nominally identical, are located next to each other, and are biased simultaneously, they work as an equivalent large single NDR device with double negative

differential conductance and capacitance. Fig. 8 (b) shows the RF equivalent circuit, where assuming RTD1 and RTD2 are identical, the total capacitance $C_n^* = 2C_n$, negative conductance $G_n^* = -2G_n$, and series resistance $R_s^* = R_s/2$. The circuit topology is similar to our previous publications [9]-[11].

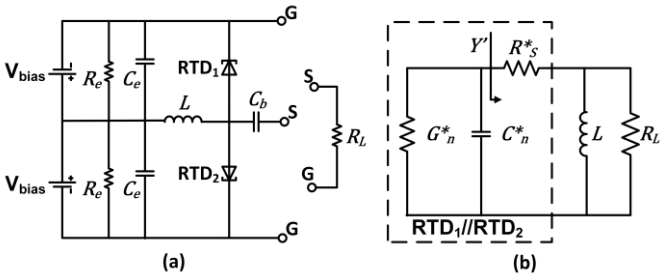

Fig. 8. (a) Schematic circuit of an oscillator employing two RTDs, each with its own DC stabilization circuit R_e and C_e. (b) Oscillator RF equivalent circuit.

The oscillator frequency f_o is determined by:

$$imag[Y'] + \omega_0 C_n^* = 0 \tag{8}$$

where Y' is the admittance of the indicated circuit.

$$f_o = \frac{1}{2\pi L(G_L R_s + 1)} \sqrt{\frac{L}{C_n} - R_s^2} \tag{9}$$

In [29], for a single NDR oscillator, where R_s is neglected and $G_n = \frac{3\Delta I}{2\Delta V}$, when $G_L = G_n/2$, the maximum power $P_{max} = \frac{3}{16}\Delta V \Delta I$, where $\Delta V = 0.8V$ is the peak to valley voltage difference, and $\Delta I = 16.6\ mA$ is the peak to valley current difference. Similarly for double RTD, when $G_L = \frac{G_n^*}{2} = G_n$, $P_{max} = \frac{3}{8}\Delta V \Delta I = 5.0\ mW$. The RTD technology with low output power limitation can be overcome by optimizing device layer structure to maximize ΔV and ΔI [12]. The calculation is based on the assumption that R_s is negligible. When the oscillator frequency is close to the cutoff frequency, the power dissipated by R_s^* needs to be considered. In this case, it can be shown that [30]

$$P_{max}^*(f_0) = P_{max}\left(1 - \frac{G_n^2 + 4(2\pi f_0 C_n)^2}{G_n^2 + 4(2\pi f_{max} C_n)^2}\right) \tag{10}$$

Equation (10) demonstrates that when R_s is taken into consideration, the maximum output power $P_{max}^*(f_0)$ becomes a function of f_0. When the RTD device conductance is $-G_n = -35.6\ mS$ and the oscillation frequency $f_o = 84\ GHz$, the estimated maximum power is about 3.5 mW.

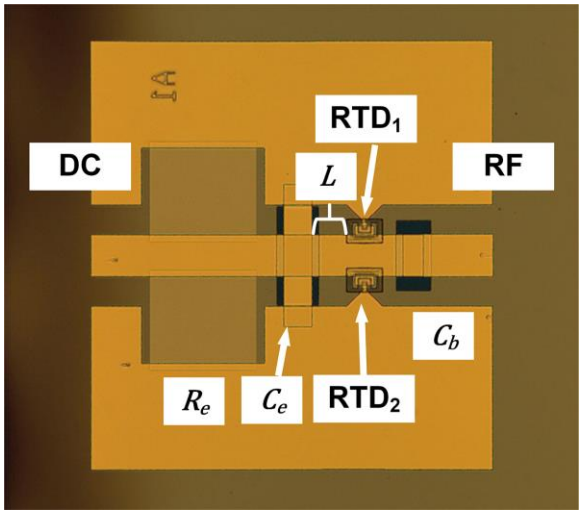

Fig. 9. Fabricated double RTD oscillator. 2RTDs are connected in parallel. Each device is biased individually with resistor R_e and bypass capacitor C_e. C_b is the DC block capacitor. The CPW length l =42 μm.

A micrograph of the fabricated circuit is shown in Fig. 9. Two RTD devices (RTD1 and RTD2) were employed in parallel in the circuit with each device biased individually. R_e was realized as a thin film NiCr resistor. The decoupling capacitor C_e was fabricated by using metal-insulator-metal (MIM) capacitor (C_e = 2 pF), with its dielectric layer SiN_x deposited by inductively coupled plasma (ICP) chemical vapor deposition (CVD). C_b was designed as a DC block capacitor with value C_b = 1.5 pF. The coplanar waveguide (CPW) structure with length of $l = 42\ um$ is terminated by C_e as shown in Fig. 9. From transmission line theory, it is known that the equivalent inductance is given by (11) where Z_0 = 50 Ω, is the CPW characteristic impedance and β is the wave number.

$$L = \frac{Z_0 \tan(\beta l)}{2\pi f_0} \tag{11}$$

A test structure was fabricated alongside the oscillator to verify the inductance value. The passive CPW test structure shown in Fig. 10 (a) and is the same design as the one integrated in the oscillator circuit. The inductance value was extracted from S-parameter measurements. As shown in Fig. 10 (b), the calculated value shows fair matching with the measurement. When $f_0 = 84\ GHz$, the extracted inductance value is 12.5 pH while the model value shows 16.3 pH.

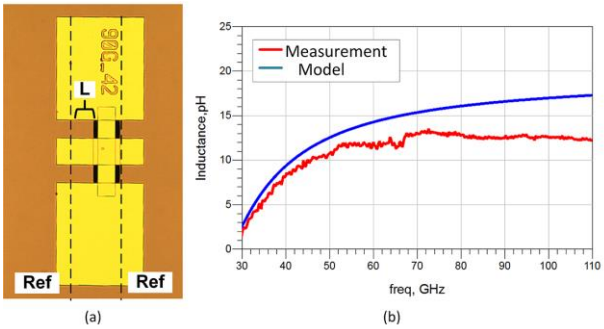

Fig. 10. (a) Passive CPW structure is the same as in oscillator design. (b) The comparison of measured and modeled inductance of the CPW structure.

The oscillators were measured on-wafer. The schematic and lab measurement setup are shown in Fig. 11 (a) and (b). Since the Keysight E4448A spectrum analyser is limited to measuring spectra up to 50 GHz, an external W-band mixer Keysight 11970W was used to down-convert the high frequency signal to the measurement range of the E4448A. As the mixer insertion loss is difficult to calibrate in the experiment, the actual power was confirmed by using Erickson PM5 power meter from VDI.

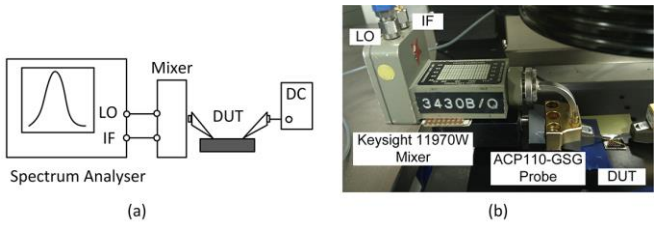

Fig. 11. (a) Schematic measurement setup. The output is through RF probe connected with external mixer to spectrum analyser. (b) Lab measurement setup. The RF probe used is Cascade ACP-110 probe. The mixer used is Keyssight 11970W mixer.

The measurement results including bias dependent frequency and power are plotted in Fig. 12. The central frequency is around 84.5 GHz, with a tunable range of about 150 MHz and a measured maximum power about 2 mW. This is the highest power reported by an RTD oscillator in the W-band range.

Using the measured oscillation frequency, the extracted contact resistance and the known resonating inductance in equation (8), the device capacitance of a single RTD can be estimated to be 78 fF. This is slightly higher than that computed from equation (1), but showing the modelling is fairly accurate.

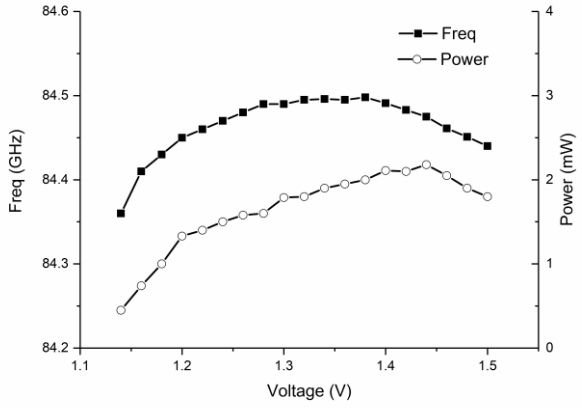

Fig. 12. Measured W-band RTD oscillator bias dependent frequency and output power. The frequency was about 84.5 GHz. The maximum power was about 2 mW.

IV. Wireless Measurements

A. Measurement set up and results

A block diagram of the measurement setup for the wireless experiments is shown in Fig. 13 (a) while the lab measurement setup is shown in Fig 13 (b). The distance between the transmit and receive horn antennas was 50 cm. The 2^{15}-1 PRBS (pseudo-random binary sequence) data from Keysight M8040A is superimposed through bias-T on DC bias of the RTD transmitter. The corresponding modulated output is transmitted through the on-wafer RF probe terminated with horn antenna (Tx). On the Rx side, the data is demodulated by zero bias Schottky barrier diode (SBD) from VDI. The typical responsivity of SBD is 2V/mW. The output is amplified by LNA with 20 GHz bandwidth and 12 dB gain. Eye diagrams of the transmitted data were investigated by 86100C oscilloscope from Keysight Technologies.

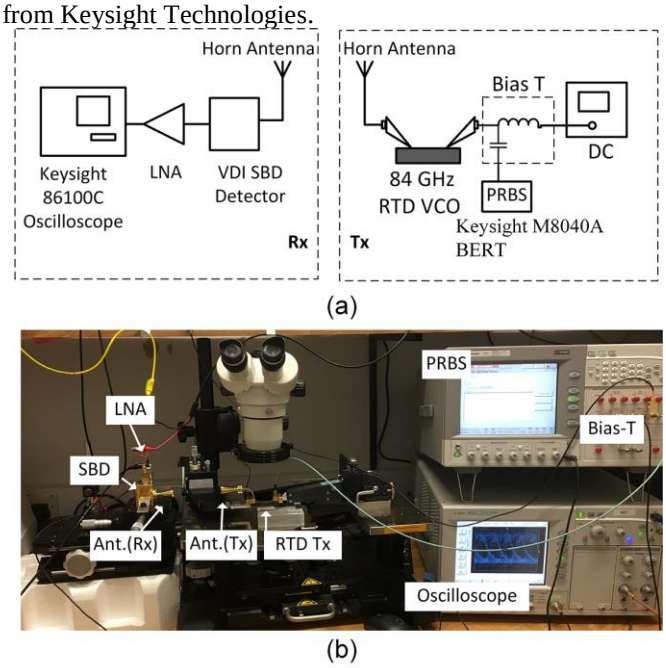

Fig. 13. (a) Block diagram of the wireless communication measurement setup (b) Measurement setup in the lab.

1) ASK modulation

When the RTD is biased at 1.3V (88mA), the best results are obtained when data amplitude ranges between -200 mV and 200 mV. From the DC characteristics shown in Fig. 4, it is known that 1.3±0.2V still corresponds to the NDR region. The measured 10 Gbps and 15 Gbps eye diagrams are shown in Fig. 14 and 15. The system's DC power consumption for the transmitter side is 114.4 mW and 613 mW for the LNA on the receiver.

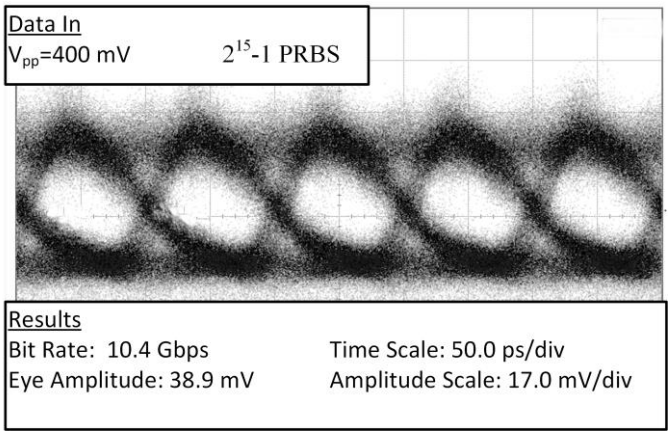

Fig. 14. 10 Gbps ASK eye diagram: when RTD is based at 1.2 V with data amplitude 400 mV.

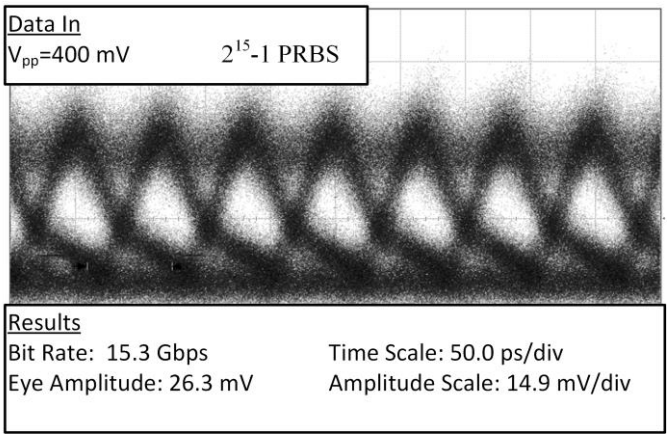

Fig. 15. 15 Gbps ASK eye diagram: when RTD is based at 1.2 V with data amplitude 400 mV.

The bit error rate (BER) was also measured using a M8040A BERT from Keysight Technologies. The results are shown in Fig. 16. Up to 5 Gbps, the BER is around 1.0×10^{-6}, 3.6×10^{-4} for 10 Gbps, and 4.1×10^{-3} for 15 Gbps. An error free BER is expected up to 10 Gbps by optimizing measurement setup such as using a high gain LNA/Antenna.

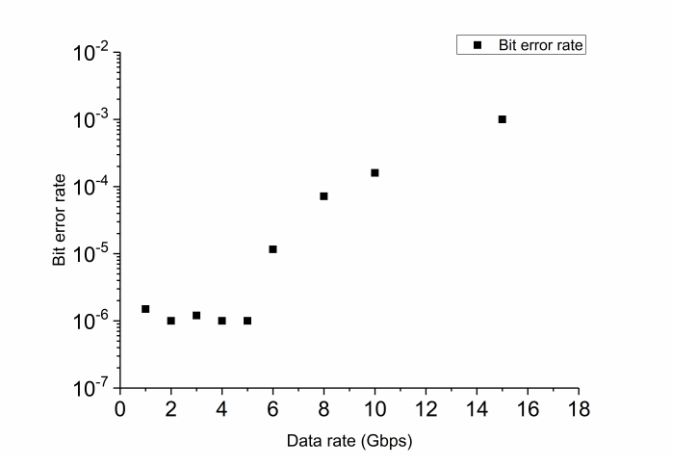

Fig. 16. Measured BER performance, Up to 5 Gbps, the BER is around 1.0×10^{-6}, 3.6×10^{-4} for 10 Gbps, and 4.1×10^{-3} for 15 Gbps.

2) OOK modulation

When the RTD was biased at 1.10V (83mA), with a data amplitude ranging from -450 mV to 450 mV, we know from Fig. 4 (device IV characteristics) that 1.1+0.45V is close to the valley voltage (on-state) while 1.1-0.45V is in positive resistance region (off-state), therefore the transmitter works in OOK mode. The measured eye diagrams of 10 Gbps is shown in Fig. 17. Compared with ASK modulation, OOK modulation shows worse performance (noisy and high BER) than ASK modulation

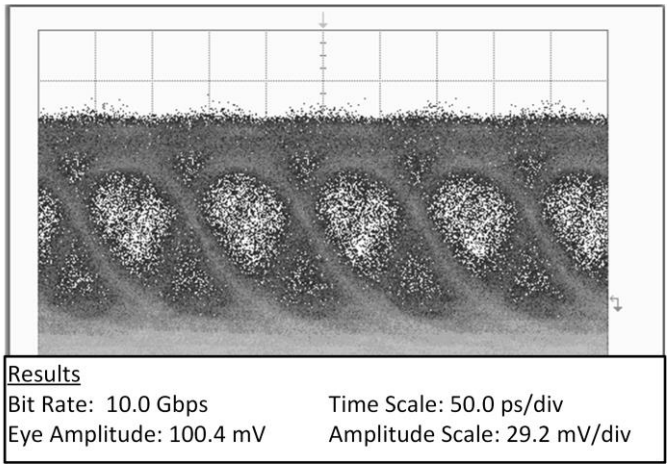

Fig. 17. 10 Gbps OOK eye diagram: when RTD is based at 1.1 V with data amplitude 900 mV.

V. Conclusion

A high-power W-band RTD oscillator/transmitter is presented in this paper. Up to 15 Gbps ASK modulation over 50 cm wireless link has been demonstrated with correctable BER. The RTD transmitters provides a very promising simple, low cost, compact solution for future ultra-fast wireless communication systems. Future work will include the integration of on-chip high gain antennas for very short range (cm ranges) applications such kiosk-downloading, or the implementation of substrate-in-waveguide technology for longer range (tens of metres) applications such as wireless links in data centers. Clearly, the use of higher modulation schemes such as QAM would enable higher data rates and so will be assessed. Also, more work on the modelling of the device is required.

Acknowledgment

The authors thank the staff of the James Watt Nanofabrication Centre (JWNC) at the University of Glasgow for help in fabricating the devices.

References

[1] P. Smulders, "The road to 100 Gb/s wireless and beyond: Basic issues and key directions," *IEEE Commun. Mag.*, vol. 51, no. 12, pp. 86–91, 2013.

[2] T. Kürner and S. Priebe, "Towards THz communications - Status in research, standardization and regulation," *J. Infrared, Millimeter, Terahertz Waves*, vol. 35, no. 1, pp. 53–62, 2014.

[3] H. J. Song and T. Nagatsuma, "Present and future of terahertz communications," *IEEE Trans. Terahertz Sci. Technol.*, vol. 1, no. 1, pp. 256–263, 2011.

[4] T. Maekawa, H. Kanaya, S. Suzuki, and M. Asada, "Oscillation up to 1.92 THz in resonant tunneling diode by reduced conduction loss," *Applied Physics Express*, vol. 9, no. 2, p. 24101, 2016.

[5] N. Oshima, K. Hashimoto, D. Horikawa, S. Suzuki, and M. Asada, "Wireless data transmission of 30 Gbps at a 500-GHz range using resonant-tunneling-diode terahertz oscillator," *IEEE International Microwave Symposium Digest*, 2016.

[6] N. Oshima, K. Hashimoto, S. Suzuki, and M. Asada, "Wireless data transmission of 34 Gbit/s at a 500-GHz range using resonant-tunnelling-diode terahertz oscillator," *Electronics Letters*, vol. 52, no. 22, pp. 1897–1898, 2016.

[7] L. Ohlsson and L. E. Wernersson, "A 15-Gb/s wireless on-off keying link," *IEEE Access*, vol. 2, pp. 1307–1313, 2014.
[8] L. Ohlsson, D. Sjöberg and L. E. Wernersson, "Codesign of Compact III–V Millimeter-Wave Wavelet Transmitters With On-Chip Antennas," *IEEE Transactions on Microwave Theory and Techniques*, vol. 66, no. 1, pp. 273-279, Jan. 2018
[9] J. Wang, L. Wang, C. Li, B. Romeira, and E. Wasige, "28 GHz MMIC resonant tunnelling diode oscillator of around 1mW output power," *Electronics Letters*, vol. 49, no. 13, pp. 816–818, 2013.
[10] J. Wang et al., "MMIC resonant tunneling diode oscillators for THz applications," *11th Conference on Ph.D. Research in Microelectronics and Electronics (PRIME)*, pp. 262-265, 2015.
[11] J. Wang, K. Alharbi, A. Ofiare, H. Zhou, A. Khalid, D. Cumming, and E. Wasige, "High performance resonant tunneling diode oscillators for THz applications," *IEEE Compound Semiconductor Integrated Circuit Symposium (CSICS)*, pp. 1-4. 2015.
[12] J. Wang *et al.*, "High performance resonant tunneling diode oscillators as terahertz sources," *European Microwave Conference*, pp. 341–344, 2016.
[13] J. Lee, Y. Chen, and Y. Huang, "A low-power low-cost fully-integrated 60-GHz transceiver system with OOK modulation and on-board antenna assembly," *IEEE J. Solid-State Circuits*, vol. 45, no. 2, pp. 264–275, 2010.
[14] C. W. Byeon, C. H. Yoon, and C. S. Park, "A 67-mW 10.7-Gb/s 60-GHz OOK CMOS transceiver for short-range wireless communications," *IEEE Trans. Microw. Theory Tech.*, vol. 61, no. 9, pp. 3391–3401, 2013.
[15] K. Nakajima *et al.*, "23Gbps 9.4pJ/bit 80/100GHz band CMOS transceiver with on-board antenna for short-range communication," *IEEE Asian Solid-State Circuits Conf.*, pp. 173–176, 2015.
[16] Y. Tanaka *et al.*, "A versatile multi-modality serial link," *IEEE Int. Solid-State Circuits Conf.*, vol. 55, pp. 332–333, 2012.
[17] A. Al-khalidi, K. Alharbi, J. Wang, and E. Wasige, "THz Electronics for data centre wireless links - the TERAPOD project," *9th Int. Congr. Ultra Mod. Telecommun. Control Syst.*, pp. 445–448, 2017.
[18] J. Davies, *The Physics of Low-Dimensional Semiconductors*. Cambridge University Press, 1998.
[19] B. B. Purkayastha and K. K. Sarma, *A Digital Phase Locked Loop based Signal and Symbol Recovery System for Wireless Channel*. Springer, 2015.
[20] J. L. Hesler, T. W. Crowe, and V. Diodes, "Responsivity and noise measurements of zero-bias Schottky diode detectors," *18th Int. Symp. Sp. Terahertz Technol.*, pp. 89–92, 2007.
[21] E. R. Brown, O. . McMahon, L. J. Mahoney, and K. . M. Molvar, "SPICE model of the resonant-tunnelling diode," vol. 32, no.10, pp. 938–940, 1996.
[22] Q. Liu, A. Seabaugh, P. Chahal, and F. J. Morris, "Unified AC model for the resonant tunneling diode," *IEEE Trans. Electron Devices*, vol. 51, no. 5, pp. 653–657, 2004.
[23] R. Lake and J. Yang, "A physics based model for the RTD quantum capacitance," *IEEE Trans. Electron Devices*, vol. 50, no. 3, pp. 785–789, 2003.
[24] E. R. Brown, C. D. Parker, and T. C. L. G. Sollner, "Effect of quasibound-state lifetime on the oscillation power of resonant tunneling diodes," *Appl. Phys. Lett.*, vol. 54, no. 10, pp. 934–936, 1989.
[25] M. N. Feiginov, "Does the quasibound-state lifetime restrict the high-frequency operation of resonant-tunnelling diodes?," *Nanotechnology*, vol. 11, pp. 359–364, 2000.
[26] M. Asada, S. Suzuki, and N. Kishimoto, "Resonant tunneling diodes for sub-terahertz and terahertz oscillators," *Jpn. J. Appl. Phys.*, vol. 47, no. 6R, p. 4375, Jun. 2008.
[27] S. Diebold *et al.*, "Modeling and simulation of terahertz resonant tunneling diode-based circuits," *IEEE Trans. Terahertz Sci. Technol.*, vol. 6, no. 5, pp. 716–723, 2016.
[28] M. Asada and S. Suzuki, "Compact THz oscillators with resonant tunneling diodes and application to high-capacity wireless communications," *ICECom 2013 - Conf. Proc. 21st Int. Conf. Appl. Electromagn. Commun.*, pp. 1–5, 2013.
[29] C. S. Kim and A. Brandli, "High-frequency high-power operation of tunnel diodes," *IRE Trans. Circuit Theory*, vol. 8, no. 4, pp. 416–425, 1961.
[30] F. C. Woo, *Principles of Tunnel Diode Crictuis*. Wiley, 1964.

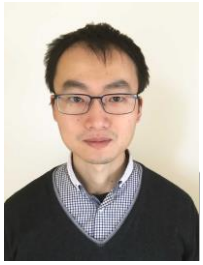

Jue Wang received the PhD degree in Electronics and Electrical Engineering from the University of Glasgow in 2014. From 2014 until now, he has been working on resonant tunneling diode based terahertz oscillator design as a postdoctoral researcher. His current research interests include high power terahertz devices and terahertz applications including wireless communications, imaging, etc.

Abdullah Al-Khalidi received his bachelor's degree, MSc and PhD degrees from the University of Glasgow in 2010, 2011 and 2015, respectively. He is currently working as a postdoctoral researcher at the University of Glasgow. His main research interest is in THz resonant tunnelling diodes (RTDs) and gallium nitride (GaN) transistor technologies.

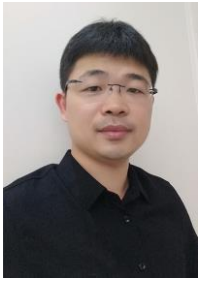

Liquan Wang (S'11–M'12) received the B.Eng. degree in Telecommunication Engineering in 2004 from Hangzhou Dianzi University, Hangzhou, China, and the M.Sc. degree and the Ph.D. degree in Electronics and Electrical engineering from the University of Glasgow, Glasgow, U.K., in 2006 and 2012, respectively.
Since 2012, he has been with Shanghai Electro-mechanical Engineering Institute, Shanghai, China. His research interests include reliable design of high-power resonant-tunneling-diode (RTD)-based microwave and THz oscillators, RTD-driven laser diode circuits and associated applications, and the development of THz imaging systems.

Razvan Morariu received the M.Eng. degree in Electronics and Electrical Engineering in 2016 from the University of Glasgow, Glasgow, U.K., where he is currently working towards the Ph.D. degree in the design and characterization of resonant tunneling diode (RTD)-based terahertz oscillators and detectors.

Afesomeh Ofiare received the BEng degree in Electrical and Electronic Engineering from Madonna University, Nigeria in 2005, and received the MSc and Ph.D. degrees in Electronic and Electrical Engineering from the University of Glasgow, UK in 2009 and 2016 respectively. He is currently a Research Assistant at the University of Glasgow. His present research interests include high-frequency device characterisation, antennas for millimetre-wave and THz applications and wireless communications.

Edward Wasige received the BSc. (Eng.) degree in Electrical Enigineering from the University of Nairobi, Kenya, in 1988, the MSc.(Eng.) from the University of Liverpool (UK) in 1990, and the PhD degree in Electrical Engineering from Kassel University (Germany) in 1999. Prior to becoming a Lecturer at the University of Glasgow in 2002, he was a UNESCO postdoctoral fellow at the Technion – Israel Institute of Technology. His current research interests include compound semiconductor micro/nanoelectronics and applications with focus on GaN electronics and RTD-based terahertz electronics.